Abundant α-Synuclein compact dimers

Sofia Zaer[‡1], Paz Drori[‡1], Mario Lebendiker[§], Yair Razvag[‡], Eitan Lerner[‡2]

From the [‡]Department of Biological Chemistry, The Alexander Silberman Institute of Life Sciences, Faculty of Mathematics & Science, The Edmond J. Safra Campus, The Hebrew University of Jerusalem, Jerusalem 9190401, Israel; [§]Wolfson Centre for Applied Structural Biology, The Alexander Silberman Institute of Life Science, Faculty of Mathematics & Science, The Edmond J. Safra Campus, The Hebrew University of Jerusalem, Jerusalem 9190401, Israel.

Running title: *αSyn dimers are abundant*

[1]Both authors contributed equally to this work.

[2]To whom correspondence should be addressed: Eitan Lerner: Department of Biological Chemistry, The Alexander Silberman Institute of Life Sciences, Faculty of Mathematics & Science, The Edmond J. Safra Campus, The Hebrew University of Jerusalem, Jerusalem 9190401, Israel; eitan.lerner@mail.huji.ac.il; Tel.+972-2-6585457.

Keywords: Parkinson's disease (PD), α -synuclein (αSyn), dimerization, oligomerization, chromatography, anion exchange (AIEX), Multi angle light scattering (MALS), hydrodynamic radius, Förster resonance energy transfer (FRET), Fluorescence correlation spectroscopy (FCS)

Abstract

α-Synuclein (αSyn) is an intrinsically disordered protein that forms oligomers and fibrils associated with Parkinson's disease. As such, the mechanism of its oligomerization and its possible links to neurotoxicity have been the focus of many studies. Out of the numerous oligomer types, dimers are the smallest oligomers of aSyn that have been reported. As such, αSyn dimers serve as the earliest steps in the nucleation of αSyn oligomers and later fibrils. Therefore, it is important to characterize αSyn dimers. The identification of αSyn dimers in ensemble-averaged measurements without the use of chemical modifications have been difficult, due to their apparent low abundance. Using analytical anion exchange chromatography coupled to multi angle light scattering as well as to dynamic light scattering, we show that recombinant αSyn is in equilibrium between different types of monomers and compact dimers, and that both are abundant. Additionally, bulk Förster resonance energy transfer (FRET), fluorescence cross-correlation spectroscopy (FCCS) of FRET and pulsed-interleaved excitation single-molecule FRET (PIE smFRET) measurements of mixtures of donor- and acceptor-labeled αSyn. These measurements indicated a dimer dissociation constant of 1.75 μM. We concluded that αSyn dimers exist as abundant species in equilibrium with monomers only if produced to reach concentrations of hundreds of nanomolar or above.

Introduction

α-Synuclein (αSyn) is a protein found predominantly at the presynaptic terminals of dopaminergic neurons at the *Substantia Nigra*(1, 2). In the brain, αSyn helps in maintaining the high frequency of neurotransmitter release by supporting fast and efficient formation of the soluble N-ethylmaleimide-sensitive factor attachment protein receptor (SNARE) complex(3). αSyn, however, is mostly famous for its link to Parkinson's disease (PD)(1, 4, 5) as well as other diseases and conditions(2, 5–7). One of the hallmarks of PD in dopaminergic neurons is the formation of intracellular Lewy bodies containing mostly aggregates of αSyn(2, 4).

αSyn is a 140 amino acid protein exhibiting large amplitude structural dynamics(8) that lacks a well-defined structure in physiological solution. The protein is divided into three domains: i) the N-terminal domain (amino acids 1-60), ii) the non-amyloid-β component (NAC; amino acids 61-95) and iii) the C-terminal domain (amino acids 96-140). αSyn spontaneously oligomerizes into various forms,

ultimately leading to its irreversible aggregation and fibrillization. Although for many years, the deposits of αSyn fibrils found in PD brains have been the possible molecular link to the disease, it has become clear in the last decades that certain αSyn oligomers, rather than aggregates, induce neurotoxicity(9). This is the reason why it is important to study the mechanism by which αSyn oligomerizes. From the structural aspect in the membrane the N-terminal and NAC domains adopt an α-helical structure(10, 11) as a monomer that switches conformations as a function of membrane curvature(12). Additionally, it can form many other structures as oligomers of different sizes either when in solution or when embedded in the membrane, including ones that can lead to membrane disruption, cellular toxicity(13) and to form membrane pores(14). Altogether, the heterogeneity of both the structures and the oligomer sizes of αSyn make it hard to decipher the mechanism by which it oligomerizes.

αSyn has been found in the cell predominantly as a monomer(15), although there have been reports it can also exist as a helical tetramer (16). The first step in the oligomerization of any protein is naturally the process of how it forms the oligomer with the minimal number of subunits. The αSyn oligomer with the smallest size that has been reported to occur *in Vitro* in physiological and at ambient conditions is a dimer(17–23). Additionally, it is known that an early crucial step in the development of PD is the formation of a covalent αSyn dimer under oxidative stress(24), via formation of dityrosinate linkages(25). Therefore, the initial formation of a noncovalent αSyn dimer from a monomer-dimer equilibrium might be a precursor for the dityrosinate-linked stable αSyn dimer.

From these reasons, it is important to study the mechanism by which αSyn forms a noncovalent dimer. However, because the abundance of αSyn noncovalent dimers was considered low(23), it was detected and studied either after dimers were captured via cross-linking(19, 20, 23) or by single-molecule(21, 22) and ensemble-averaged(18) techniques that do not necessarily account for the full monomer-dimer equilibrium. Knowing the dissociation constant of the noncovalent αSyn dimer would help define how to study the mechanism of the dimer formation. In this work we use anion exchange chromatography (AIEX) coupled to multi angle light scattering (MALS)(26, 27) to objectively and directly link each species eluted in a chromatographic run of αSyn to its average molecular mass. We show that the ensemble of freshly-prepared recombinant αSyn exists in an equilibrium between monomers and compact dimers with a large dimer fraction when at micromolar concentration. Additionally, the AIEX results regarding the αSyn monomer imply that it undergoes a slow change from a highly heterogeneous state to a less heterogeneous and more compact monomer species. We performed intermolecular Förster resonance energy transfer (FRET) experiments using steady-state fluorescence, time-resolved fluorescence, fluorescence cross-correlation spectroscopy (FCCS) and pulsed-interleaved excitation (PIE) single-molecule FRET (smFRET) to show the abundance of the dimer relative to the monomer concentration.

Results

Wild-type αSyn consists of more than monomers

We began by preparing recombinant wild-type (WT) α-Synuclein (αSyn) by expression in *Escherichia coli* and extraction from the periplasm by osmotic shock(28, 29) and ammonium sulfate precipitation yielding a highly pure protein (see *Experimental Procedures*). After the protein samples have been prepared, we further tested them for purity using anion exchange chromatography (AIEX; MonoQ, GE Healthcare). Both denaturing (SDS) and non-denaturing (native) polyacrylamide gel electrophoresis (PAGE) indicate the protein sample is pure with bands indicative of αSyn monomers and no indication of dimers (Fig. S1). Additionally, mass spectrometry characterization of molecular mass of the intact protein reports on the exact molecular mass of the protein sample, with no indication of a dimer (Fig. S2). We expected, however, that any noncovalently-formed complex to be dissociated in the conditions used for molecular mass determination using mass spectrometry (see *experimental*

procedures). Additionally, we also suspected that the determination of molecular species using PAGE could be insufficient. We hence sought out for methods that will yield a direct readout of the mass of different oligomeric species in solution, with minimal chemical modifications or perturbations.

AIEX allows probing different elution peaks in chromatography based on their ionic strength values. Coupling analytical AIEX chromtography to multi angle light scattering (MALS; see *Experimental Procedures*) allows probing different elution peaks for their molecular mass directly, rather than via transformation from its hydrodynamic radius (R_H) or its radius of gyration (R_G) (26, 27, 30). In addition to the MALS system, a quasi-elastic light scattering module also allowed measuring dynamic light scattering (DLS) curves, from which the values of R_H were retrieved, in addition to and independent of the molecular mass estimation. We performed AIEX chromatography on the WT αSyn sample (Fig. 1, A). Coupling AIEX to MALS yielded a single elution peak having a molecular mass of 21.6±0.8 kDa (Fig. 1, B; Table S1), which was a clear deviation from the expected molecular mass of 14.4 kDa (Fig. 1, B, lower dotted line). Additionally, the DLS-derived R_H value was 53.3±0.9 Å (Table S1). Previous studies have reported R_H values of 32-34 Å for αSyn(31, 32), as well as values larger than that(33, 34). Additionally, an αSyn monomer (molecular mass of 14.4 kDa) that is unfolded may have an R_H value larger by a factor of ~3.5, relative to a well-folded protein of the same molecular mass. That estimation stems from the dependence of R_H on the molecular mass to the power of 1/3 in folded proteins(35), and its dependence on the molecular mass multiplied by 0.6 in unfolded proteins(36). This may have served as an explanation for the R_H value if the MALS-derived molecular mass was close to 14.4 kDa. The value of the molecular mass, however, was larger (21.6±0.8 kDa).

We hypothesized that the elution peak consisted of a mixture of αSyn monomers and dimers, where both have only little difference in their ionic strength values. This possibility may explain why in AIEX, we collected a single elution peak with an average molecular mass between that of a monomer and a dimer (Fig. 1, B, dotted lines). We tried to gain information regarding the validity of the monomer-dimer mixture hypothesis by coupling size exclusion chromatography (SEC; superdex 75) to MALS(26). In the SEC-MALS chromatogram we identified two elution peaks (Fig. S3). The early elution peak had minimal absorption at λ=280 nm and intense light scattering intensity, characteristic of large molecular mass aggregates (estimated by MALS to be >1,000 kDa). The late elution peak had an average molecular mass value of corresponding to a protein the size of an αSyn dimer (30.4±0.9 versus 28.8 kDa; Fig. S4 & Table S1). The elution volume relative to a protein molecular mass calibration curve fitted to an average molecular mass of~46 kDa (32-62 kDa, according to 95% confidence bands; Fig. S4) using a calibration with well-folded proteins, which is similar to the values reported by others using SEC of αSyn(32, 37) as well as with other techniques(31, 34). These values could have been explained by an unfolded αSyn monomer, if the MALS-derived molecular mass value was close to 14.4 kDa. The value of the molecular mass, however, was twice that value (Table S1). Therefore, instead of being described by an unfolded-monomer, the elutant can be described by either an αSyn dimer, a mixture of αSyn monomers and dimers or a mixture of αSyn monomers and oligomers of different sizes. In the latter case, the different oligomer sizes should elute at different elution volumes if the size difference between them was large. We, on the contrary, identified a single elution peak with this MALS-derived molecular mass. SEC-MALS might not have the resolution to resolve αSyn monomers from dimers.

Resolving the αSyn monomer-dimer equilibrium in AIEX-MALS using Cysteine mutants

To tackle the lack of large differences in ionic strengths between the hypothesized monomers and dimers, we decided to perform the same experiments using single cysteine (Cys) mutants. We suggested that a monomer with a single Cys residue and a dimer with two Cys residues would introduce the required ionic strength difference between the two species. The

possible ionic strength difference between the species would exhibit an AIEX-MALS chromatogram where both separate well and identified as monomers and dimers according to the MALS readout. In addition, the Cys mutations used here were planned for fluorescent dye labeling in single-molecule fluorescence measurements, via thiol reactions.

We initiated our experiments using the αSyn Y39C mutant. As in the WT αSyn case, also the Y39C mutant did not show any sign of dimerization in SDS- as well as in native PAGE (Fig. S5). Analytical AIEX-MALS runs on purified Y39C αSyn have shown two clear elution peaks (Fig. 2, A, B): (i) the first elutant (lower NaCl concentration) had a molecular mass of characteristic of an αSyn monomer, and (ii) the second elutant (higher NaCl concentration) had a molecular mass of characteristic of an αSyn dimer (see Table S1). Additionally, the DLS-derived R_H values of these elutants were 30.0±0.1 and 39.0±0.3 Å, respectively (see Table S1). The R_H value of the elutant characteristic of an αSyn monomer has also been reported in previous reports as the value for the αSyn monomer(31, 32). The R_H value of the elutant characteristic of an αSyn dimer, however, does not represent a significant change relative to the R_H value of an αSyn monomer. This implies that the αSyn dimer is relatively compact. Moreover, the elution peak characteristic of an αSyn monomer was wide and heterogeneous, as might be expected from an un-structured protein, exposing many different possible charged groups. The elution peak characteristic of the dimer, however, had a clean shape characteristic of a species with a homogeneous ionic strength distribution. We then re-injected the freshly-eluted monomer and dimer species, to test the reversibility between them (Fig. 2, green- and magenta-labeled elution volume ranges). The αSyn monomer forms a mixture of chromatographically-separated monomer and dimer elutants, in about an hour (Fig. 2, C; molecular mass values in Table S1) and with R_H values of 22.8±0.9 and 25.8±1.8 Å, respectively (Table S1). Interestingly, the dimer breaks down to monomers as well (Fig. 2, D; molecular mass values in Table S1). This result emphasizes the reversibility of a dimer back to a monomer, expected in dynamic equilibrium. Judging by the ratio of the areas of the eluted fractions between the monomer and the dimer peaks, before and after dimer re-injection, it seems that the dimer dissociates back to monomers slowly. Conversely, due to the lack of thiol reducing agent in the elution samples, we anticipated that a covalently-bound dimer would eventually form due to disulfide bridges, in addition to the noncovalent dimers. Still, if disulfide bridge formation would have been efficient, we would not have observed the αSyn monomer dissociates back from the αSyn dimer species. Concluding the findings summarized in figure 2: there exists a slow (minutes scale) exchange between αSyn monomers and noncovalently-formed dimers.

We also noticed that the elution volumes of the monomeric αSyn elutant in the re-injection experiments (Fig. 2, C, D, left shades) were comparable to the high elution volume edge of the wide elution volume range of the αSyn monomer elutant (Fig. 2, B, green-labeled elution volume). The re-injected αSyn dimer elutant, however, was eluted at volumes (Fig. 2, C, D, right shades) almost the same as the αSyn dimer species (Fig. 1, B, magenta-labeled elution volume). These results imply that the variety of αSyn monomers undergo a transition to a monomeric species exhibiting higher mean ionic strengths having a narrower distribution of ionic strength values. This is also consistent with the DLS-derived R_H values. While the R_H value of the αSyn monomer elutant (Fig. 2, B, green-labeled elution volume) was 30.0±0.1 Å, its value in the re-injection experiments was 22.8±0.9 Å (see Table S1). Notably, the reinjection experiments have been performed in intervals of one hour. Overall, we have identified a slow transition of the αSyn monomers from a conformationally-heterogeneous state to a conformational state with higher compactness.

As control experiments, we performed AIEX-MALS on the Y39C αSyn mutant in two other conditions that should prevent disulfide bridge formation: AIEX-MALS (i) in the presence of β-mercaptoethanol (βME; Fig. S6, A) and (ii) on the Y39C mutant after the thiol of its Cys group has been blocked by an acetamide group, following coupling to iodoacetamide

(IAA; Fig. S6, B). In both tests we report major and minor elution peaks, where the MALS-derived molecular mass of the minor elution peak is higher than 1,000 kDa characteristic of large oligomers and aggregates. In both tests, the major elution peaks had molecular mass values significantly larger than the monomer molecular mass (see Table S1). These results were analogous to the results we found for the WT αSyn (Fig. 1), where no monomer-dimer separation was observed. Additionally, in these conditions, the ionic strength differences between the monomer and the dimer species were canceled, which explains why in AIEX the major elution peak has the same elution volume. However, the values of the hydrodynamic radii of the major lution peaks in these tests (see Table S1) were much smaller than the values we recorded for the WT αSyn and also smaller relative to the usual values measured for αSyn (~30 Å(31, 32)). This means that although the ionic strength difference was canceled, the single elution peaks can be well-described by a mixture of compact monomers and dimers.

To test whether the AIEX-MALS results for the Y39C αSyn mutant were a special case of this mutation, we tested other αSyn single Cys mutants. The A56C αSyn mutant, for instance, gave similar results (Fig. S7 & Table S1) similar to the ones given for the Y39C mutant (Fig. 2), namely: (i) lower NaCl concentration eluted peak characteristic of a compact αSyn monomer, (ii) higher NaCl concentration eluted peak characteristic of a compact αSyn dimer, (iii) re-injected monomer elutant yields separation into a more compact monomer elution peak as well as a dimer elution peak, (iv) the same is true for the re-injected dimer elutant, although with different monomer-dimer elution peak ratios (the amplitude of the re-eluted monomer species is lower than in Y39C in Fig. 2, D) and (v) the eluted monomer after re-injection of either the monomer or dimer elutants is eluted at a volume range that fits the edge of the elution volume range in the first run (Fig. S7, compare the left shades in panels B & C to the green region-of-interest in panel A). As for the dimer, its elution volume range stays the same in all runs. Additionally, the R_H values of the monomer elutant after re-injection are smaller than before re-injection.

In summary, we gained strong basis for our hypothesis that αSyn forms an abundant noncovalent dimer species that is compact and in complex equilibrium with different types of αSyn monomers. However, as it is an intermolecular interaction, the abundance of the dimer should depend on the monomer concentration. The question is to what extent? To answer this question, we utilized Förster resonance energy transfer (FRET) for identifying the abundance of αSyn dimerization. For that, we labeled the thiol group in the Cys of the Y39C mutant with either ATTO 488 or ATTO 647N as donor or acceptor dyes, respectively (see *Experimental Procedures*).

αSyn dimers are abundant in micromolars

We started by performing bulk FRET measurements of a mixture of donor- and acceptor-labeled αSyn, using excitation spectra, focusing on the acceptor fluorescence intensity at λ=665 nm (Fig. S8, blue). As a control, we also recorded the acceptor excitation spectrum of a sample that included only an acceptor-labeled αSyn (Fig. S8, black). The acceptor excitation spectra were normalized by the wavelength range applicable to direct acceptor excitation (525-650 nm). In the wavelength range applicable to donor excitation (440-525 nm), spectra intensities are indicative of the involvement of molecular complexes in the sample in FRET (acceptor excitation indirectly through donor excitation accompanied by energy transfer). Freshly-prepared singly-labeled αSyn samples should include mostly monomers and if any dimers or oligomers exist, they will yield only a minimal FRET signature in bulk intermolecular FRET measurements. This is because most αSyn molecules have not yet oligomerized. Indeed, the results show that in a freshly-prepared sample of 100 nM mixture of donor- & acceptor-labeled αSyn, a nonnegligible amount of acceptor-labeled αSyn can be excited by donor-labeled αSyn via donor excitation accompanied by FRET, which can occur only in dimers or larger oligomers (Fig. S8, blue compared to black). As a positive control to show that αSyn eventually oligomerizes, we performed the acceptor excitation spectra

recordings on these samples, after 20 hour shaking in T=37°C. By that, we expected to identify larger fluorescence excitation via FRET, due to a larger portion of αSyn proteins involved in dimers and oligomers. Indeed, the fluorescence intensity at λ=665 nm following excitation in the wavelength range applicable to donor excitation, increased (Fig. S8, red compared to blue and to black). Therefore, the contribution of αSyn species to the overall FRET signal increases, as expected from larger oligomers involving both donor- and acceptor-labeled αSyn proteins. As for the freshly prepared αSyn samples, the qualitative signature of FRET might not necessarily arise solely from dimers. Still, judging by the results from analyses of AIEX-MALS, at concentrations higher than 100 nM, a solution of freshly-prepared αSyn should include mostly monomers and dimers.

To test the abundance of αSyn dimers at lower αSyn concentrations, we performed fluorescence correlation spectroscopy (FCS) and fluorescence cross-correlation spectroscopy (FCCS) measurements of mixtures of donor- and acceptor-labeled αSyn at different concentrations ranging from 100 nM down to 3 nM. In a mixture of donor- and acceptor-labeled αSyn monomers, if dimers or oligomers are formed, some of them will include both. This, in turn, will lead to the transfer of excitation energy from the donor to the acceptor, as the distances between the dyes will be in the range where FRET occurs (< 7.5 nm for these donor and acceptor dyes). Therefore, excitation of the donor may lead to either donor fluorescence photons detected on one detector, or acceptor fluorescence photons following FRET, detected on the second detector. Consequently, FRET species lead to acceptor photons uniquely detected by one of the detectors. Therefore, if the fluorescence cross-correlation between donor fluorescence photon detection times and acceptor fluorescence photon detection times (cross-correlation between the signals from the two detectors), is nonzero, it is indicative of the existence of a FRET species (e.g. αSyn oligomers). In FCCS-FRET measurements, oligomeric species diffusing through a Gaussian-shaped focused laser excitation volume should yield noticeable donor-acceptor fluorescence cross-correlation curves, following donor excitation (see *Experimental Procedures*). Indeed, the donor-acceptor fluorescence cross-correlation curves were noticeable, relative to the donor fluorescence autocorrelation curves at higher αSyn concentrations (Fig. 3, A). However, the donor-acceptor fluorescence cross-correlation amplitude decreased relative to the donor fluorescence autocorrelation amplitude as the αSyn concentration decreased (Fig. 3, B, C). This is indicative of a decrease in the coincidence(38) of donor- and acceptor-labeled αSyn.

In the monomer-dimer equilibrium, the concentration of the dimer species should depend on the monomer concentration to the power of two, as in Eq. 1.

$$[Dimer] = \frac{1}{K_D}[Monomer]^2 \quad (1)$$

where K_D is the dissociation constant. Plotting the dimer concentration as a function of the monomer concentration to the power of two should yield a line with a slope from which we can derive the dissociation constant. The value of the dissociation constant will exhibit at which concentrations the dimer is abundant.

The concentration of the species yielding FRET-related donor-acceptor cross correlation (C) depends on the amplitudes of the donor and acceptor auto- and cross-correlation curves according to Eq. 2(39):

$$C = \frac{G_{DA}(0)}{G_D(0)G_D(0)V_{eff}} \quad (2)$$

where $G_D(0)$, $G_A(0)$ and $G_{DA}(0)$ are the values of the donor fluorescence autocorrelation, acceptor fluorescence autocorrelation and donor-acceptor fluorescence cross-correlation curves when extrapolated to zero lag time (also known as the correlation amplitudes), and V_{eff} is the effective excitation volume formed by the detection of photons from a tightly focused Gaussian-shaped laser excitation. The value of V_{eff} was calibrated by measuring a free fluorescent dye with a known diffusion coefficient (ATTO 488 with a diffusion coefficient of ~400 $\mu m^2/s$ at a temperature of 25°C(40)), and found to be 2.0±0.1 fL.

The fluorescence correlation amplitudes were derived from fits of fluorescence curves to either of the following models: (i) the donor-

acceptor fluorescence cross-correlation curves and the acceptor fluorescence auto-correlation curves were fitted to a function describing the fluorescence correlation due to free diffusion in 3D Gaussian-shaped effective excitation volume, as in Eq. 3(41):

$$G(\tau) = \frac{G(0)}{\left(1+\frac{\tau}{\tau_D}\right)\left(1+\frac{1}{\kappa^2}\frac{\tau}{\tau_D}\right)^{1/2}} \quad (3)$$

where τ is the lag time, *G(0)* is the correlation amplitude, τ_D is the characteristic time for diffusion through the effective excitation volume and κ is the ratio between the z and x/y diameters of the Gaussian-shaped effective excitation volume, taken here to be equal to 7; (ii) as the fluorophore chosen to be the donor is ATTO 488, which exhibits also triplet blinking(42), the fluorescence auto-correlation curves of the donor were fitted to a function describing the fluorescence auto-correlation due to both free diffusion in 3D Gaussian-shaped effective excitation volume and triplet blinking, as in Eq. 4(43, 44):

$$G(\tau) = \left(1 + Te^{-\frac{\tau}{\tau_T}}\right)\frac{G(0)}{\left(1+\frac{\tau}{\tau_D}\right)\left(1+\frac{1}{\kappa^2}\frac{\tau}{\tau_D}\right)^{1/2}} \quad (4)$$

where T is a coefficient describing the bright-to-dark equilibrium constant and τ_T is the relaxation time of the triplet blinking process. An example of the fitting procedure and the retrieved correlation amplitudes for αSyn concentration of 25 nM is reported in Figure S9.

The values of the correlation amplitudes for concentrations 100, 50, 25, 12.5, 6.25 and 3 nM for the donor and acceptor fluorescence auto-correlation and the donor-acceptor fluorescence cross-correlation curves are reported in Table S2. These values were used together with the nominal concentrations of the αSyn to calculate the dimer concentration in each measurements, using Eq. 2. The results were reported in two ways: (i) the dimer fraction and (ii) the dimer vs. monomer concentrations to the power of two, from which linear fits yielded estimates of the dimer dissociation constant (Eq. 1).

At a nominal αSyn concentration of 100 nM, 5.7±0.6 % of αSyn is involved in dimers (Fig. S10). Moreover, as αSyn concentration decreases, the fraction of dimers decreases as well (down to less than 0.1 % at 3 nM αSyn concentration; Fig. S10).

Figure S11 show the results of a linear fits to the dependence of the dimer concentration on the power of two of the monomeric αSyn concentration. Then, using the conversion in Eq. 1, we find a dimer dissociation constant of 1.75±0.02 μM. Overall, the dimer dissociation constant is in the micromolars, which explains why in high αSyn concentrations required for AIEX-MALS, we identify abundant αSyn dimers. However, at a few nanomolar concentration or lower, the abundance of the αSyn dimers is negligible.

The fluorescence correlation curves of the mixtures of donor- and acceptor-labeled Y39C αSyn mutant were taken using pulsed laser excitations and with detectors routed to a time-correlated single photon counting card. This allowed us to record photon arrival times relative to the moments of excitation, hence fluorescence decays. If a fraction of the donor- and acceptor-labeled αSyn molecules under measurement are dimers, a clear signature should appear in the donor-excited acceptor fluorescence decays. At high αSyn concentration, where the fraction of dimers showing FRET should be high, the acceptor fluorescence decay following donor excitation are expected to decay slower (longer lifetime) relative to the same decays measured at lower αSyn concentrations, when the fraction of dimers is low. Figure 4 shows exactly this trend. One can see that the acceptor fluorescence decay following donor excitation pertains even at low αSyn concentrations. This is due to the leakage of the donor fluorescence decay to the acceptor detection channel, which is low (See Fig. S12). However, the amount of molecules exhibiting FRET is also low at this concentration. Overall, the acceptor fluorescence decays following donor excitation show that the lower αSyn concentration is, the faster the curves decay (Fig. 4). The slow decay component is a hallmark of FRET occurring at high αSyn concentrations.

Directly observing αSyn dimers using single-molecule FRET

The above results that were based on FCS and on acceptor fluorescence decays, assume the contribution for FRET ariss solely from dimers and not from higher size αSyn oligomers. Based on the equilibrium observed in micromolar concentrations in AIEX-MALS involving mostly monomers and dimers, it is safe to assume the fraction of larger size oligomers will stay negligible at lower αSyn concentrations. Our goals were also to study the αSyn dimer conformations using single-molecule fluorescence-based techniques. These measurements require working concentrations of <100 pM, at which we might not observe αSyn dimers at all. We tested the performance of pulsed-interleaved excitation (PIE; or nanosecond alternating laser excitation; nsALEX) (45, 46) single-molecule FRET (smFRET) measurements of αSyn dimers measured at 100 pM. This method allows classifying single molecule populations according to them exhibiting FRET efficiency values, as well as according to their donor:acceptor stoichiometry. We expect dimers with FRET to have a 1:1 donor:acceptor stoichiometry. In PIE/nsALEX donor and acceptor excitations alternate in tens of nanoseconds, so that each single molecule that traverses the effective excitation volume (in a few milliseconds) experiences multiple donor and acceptor excitation rounds. We define the stoichiometry ratio (S) of single molecule photon bursts as the ratio of the photons arising from donor excitation and the photons arising from both donor and acceptor excitations (Eq. 5)(47, 48).

$$S = \frac{n_D^D + n_D^A}{n_D^D + n_D^A + n_A^A} \quad (5)$$

where $n_D{}^D$ and $n_D{}^A$ are the number of donor and acceptor photons, respectively, arising from donor excitation, and $n_A{}^A$ is the number of acceptor photons arising from acceptor excitation.

An αSyn dimer with a donor:acceptor stoichiometry of 1:1 will yield a population of single molecule photon bursts with S~0.5, if all correction factors were employed(48). αSyn monomers will either have one donor or one acceptor, which will yield S~1 or S~0, respectively. To overcome the anticipated low fraction of αSyn dimers at the concentrations used in PIE-smFRET (<100 pM), we performed a long measurement (one hour acquisition; Fig. 5). Indeed the majority of single molecule bursts were either donor-only or acceptor-only species with S~1 and S~0, respectively (Fig. 5, A). However, there were very few single-molecule photon bursts with S values between 0 and 1. Burst selection for bursts that had photons both when the donor was excited and when the acceptor was excited yielded the few single-molecule photon bursts that apparently had both a donor and an acceptor when diffusing through the effective excitation volume (Fig. 5, B). Note that these bursts have a variety of S values, some of which are lower than 0.5. The value deviates from 0.5 most probably because S values were not corrected for the possible imbalance in donor and acceptor fluorescence quantum yields and in their detector efficiencies (the γ factor) and for the possible imbalance in donor and acceptor excitation yields (the β factor)(48, 49). Additionally, the lack of a sufficient amount of such photon bursts makes it difficult to estimate the mean S value, accurately. Nevertheless, this result implies the few FRET species are close to the S values characterizing dimers.

Discussion

In this work, we found that the monomer-dimer αSyn equilibrium has a dissociation constant of 1.75 μM. This ultimately means that when probing a solution of freshly-prepared recombinant αSyn with a nominal concentration in the micromolars, there is a significant amount of dimers that are formed. The dissociation constant value is lower from what is considered as the critical concentration for αSyn fibril formation by an order of magnitude – 20 μM(50, 51). Therefore, this means that at a few μM concentrations, mostly short oligomers are formed, and at lower concentrations, the αSyn monomer is the predominant species.

AIEX-MALS has proved to be indispensable in reporting on the ionic strength, the molecular mass and the hydrodynamic radius of each elutant, independently(26, 27). In AIEX-MALS experiments of WT αSyn, we identified a single elution peak with a molecular mass larger

than expected from the monomer (> 14.4 kDa). Unlike in PAGE, the molecular mass in MALS is not based on the hydrodynamic radius of the material migrating in the gel. αSyn does not have a well-defined structure, which is why it may be hard to connect its band position in PAGE to the molecular mass. In MALS, the molecular mass is calculated from two direct optical readouts, namely the protein light absorption and the light scattering intensity, used in the Rayleigh scattering formula (26, 27, 30). The light scattering intensity in our experiments was independent of the shape of the scattering proteins, since the incident light wavelength, 658.9 nm, is much larger than the sizes of the scattering protein molecules. Therefore, unlike molecular mass estimations that rely on transformation from hydrodynamic radii or radii of gyration, in MALS the retrieved molecular mass values are similar to the theoretical molecular mass values. Additionally, in MALS the molecular mass is determined immediately when the protein elutes. Therefore, MALS provides a direct measure of the molecular mass. Nevertheless, since the system we used also had a quasi-elastic light scattering module, we were able to measure the hydrodynamic radii, independently, from DLS curves. A single elution peak with a molecular mass higher than expected for αSyn monomer might represent a mixture of monomer with other oligomers that together yield an average molecular mass that is larger than expected for 100% monomeric species. However, the lack of separation implies the species in the mixture do not have significant differences in their ionic strengths. In AIEX-MALS experiments of αSyn Cys mutants (Y39C and A56C), the monomer species exposing a single Cys residue had lower elution volume range values than for the dimer species exposing two Cys residues. Since in AIEX the elution volume is associated with the conductivity as a function of the NaCl gradient, different elution volumes translate to different species with different ionic strengths caused by differences in the exposed charges. Without coupling the chromatography to MALS, it would not be possible to identify deviations of that single elution peak from its expected molecular mass. It should be noted that the same procedure performed with either Cys mutants, in thiol reducing conditions or after Cys thiols were chemically-blocked, yielded single elution peak with similar molecular mass values as the ones observed for the WT αSyn. Therefore, the strategy of separation using Cys residues provided the required ionic strength differences that allowed proving the results using the WT αSyn were indeed a mixture of predominantly monomers and dimers. In addition, since many other labs routinely purify their recombinant αSyn samples and usually resolve it as a single elution peak assuming it is pure, our results show that these elutions still yield mixtures of different αSyn species.

The separation into monomers and dimers according to MALS-derived molecular masses, coupled to the knowledge of their hydrodynamic radii allowed us to gain insight about their compactness. The noncovalent αSyn dimer R_H value was found to be ~38 Å. A well-folded protein with a mass equivalent to an αSyn dimer (28.8 kDa) should have an R_H value of 20-25 Å. The dependence of R_H on the molecular mass is to the power of 1/3 in folded proteins(35), and its dependence on the molecular mass is a multiplication by 0.6 in unfolded proteins(36). Therefore a fully unfolded protein of that mass should have an R_H value larger by factor of 5.6. However, the hydrodynamic radius of the αSyn dimer was much smaller than that estimation. Therefore, the αSyn dimer is compact, but not as compact as a fully folded protein of that mass.

Re-chromatography of eluted species allowed us to show that the αSyn dimers can dissociate back to monomers. These AIEX-MALS experiments were used in the absence of thiol reducing agents. Therefore it was expected that after a enough time, dimers would covalently form via disulfide bridges. Indeed, re-chromatography of these elutants after seven hours yielded a single elution peak with a molecular mass of a dimer (data not shown). Luckily, the kinetics of disulfide bridge formation is sometimes very slow, which opens a time window to study noncovalent reversible monomer-dimer equilibrium of αSyn Cys mutants, in the absence of thiol reducing agents.

Interestingly, the characteristics of the monomer elutant change slowly. These included: i) a shift of the ionic strength distribution towards

a narrower one with a larger mean value, as well as the ii) a shift of the R_H value towards a more compact species. His trend occurred also after re-chromatography of the dimer elutant. Does this mean that the αSyn dimer helps in the transition of the monomer αSyn into a more homogeneous and compact monomeric species? If yes, this might speculatively mean that the αSyn dimer may help catalyze folding of the αSyn monomer. However, the time interval between consecutive chromatographic runs in our experiments was ~ 1 hour, in which dimer dissociation and monomer transition into a conformation with higher compactness could have occurred independently. Overall, this may imply that the monomer-dimer equilibrium in αSyn does not necessarily follow a simple two-state mechanism. Surely the herein speculation is a subject for future study. While this speculation might seem exotic at first glance, the oligomerization process might not be a simple linear process. As an example, it has already been found using an immobilized single-molecule fluorescence assay, that the αSyn dimer exists in two different forms characterized by two different lifetimes(22). Accompanied to many other reported complications, the one reported here on a possible difference between monomers and monomers that were formed after dimer dissociation might be another new complexity.

The abundance of spontaneously-formed αSyn noncovalent dimers may explain why studying αSyn dimers using chemically crosslinked proteins succeeded(19, 23). That is because crosslinking is usually performed at micromolar concentrations or higher. Importantly, higher αSyn concentrations may involve also in the formation of oligomers with larger sizes, such as trimers and tetramers(23). Additionally, the results can explain why techniques such as smFRET of freely-diffusing molecules might not work. Our PIE smFRET measurements, which require working with fluorescently-labeled proteins at a concentration lower than 100 pM, resulted in a very small population of single molecules that exhibited FRET and were probably αSyn dimers. Studying the structure of the αSyn noncovalent dimer and its conformational dynamics, when it is only one subpopulation out of many other species, is challenging using ensemble-averaged biophysical techniques. This is why single-molecule techniques are such a big promise for these studies. Zhengjian *et al.* has devised an assay in which un-labeled αSyn proteins were surface immobilized and αSyn proteins dye-labeled with a fluorescent dye flowed in the solution(22). When dimerization occurred, the fluorescence from single immobilized molecules was simply tracked until dissociation led to disappearance of the fluorescence signal. This approach allowed defining the kinetics of the dissociation. However, focusing just on dimers did not allow assessing the association kinetics. Therefore, although powerful, this single-molecule approach did not probe the whole monomer-dimer equilibrium. This approach, however, can be used in the study of the structure of the αSyn dimers using FRET, if instead of an immobilized un-labeled αSyn, an immobilized acceptor-labeled αSyn would be used. Screening through many such immobilized smFRET experiments of many combinations of donor and acceptor labeling positions will yield a list of inter-residue distance information. This set of data could be used as spatial restraints when modelling the ensemble structure of the αSyn dimer. This approach, however, still might include the chemical perturbation of surface immobilization. Another single-molecule approach that did not involve immobilization, but yielded more information on αSyn oligomers than in smFRET of immobilized proteins, was an approach in which αSyn proteins flowed in a microfluidic device in laminar flow, and the size of the oligomer was identified by the burst size, arising from the increased amount of dyes in a larger oligomer consisting dye-labeled αSyn proteins(52). This approach, however, yielded distribution of oligomer sizes, from which it was hard to decipher the information just for the dimers. Using this approach coupled to FRET allowed identifying also the mean FRET efficiency distributions for different oligomer size distributions. The addition of PIE or ALEX could have also assisted in a better determination of the oligomer size from the donor:acceptor stoichiometry ratio(45, 47).

In addition to single-molecule techniques, bulk techniques can allow measuring an abundant portion of αSyn dimers, if the

working concentration can be a few micromolars. One of these include structural determination using information drawn from crosslinking mass spectrometry (XL-MS)(53). Using crosslinkers of certain lengths, masses of certain crosslinked peptides can be traced back to which amino acids were at that distance. XL-MS is well-suited for the determination of well-organized proteins and complexes, where the distribution of inter-residue distances around the mean distance, are quite narrow. However, in crosslinked flexible peptides, two residues may reach the distance of the crosslinker length because they can probe many distances, far from their mean distance values. Therefore, XL-MS can be used in the case of a protein as flexible and heterogeneous as αSyn to resolve its structure, but the experimental results should be interpreted as probabilities to reach certain distances rather than actual representative inter-residual distances. Indeed, XL-MS coupled to discrete molecular dynamics simulations has been used to study the ensemble structure of the αSyn monomer(54). Luckily, with approaches such the Szabo-Schulten-Schulten theory(55), the crosslinker lengths can be treated as cutoff distances to which the inter-residue distance can diffuse with a certain probability. In future works, we will use the abovementioned techniques to study the ensemble structure of the spontaneously-formed noncovalent αSyn dimer.

From the biological point of view, the abundance of spontaneously-formed αSyn dimers raises questions as to the possibility for them to spontaneously form also in the cell. αSyn dimers may well be formed also as a reaction to specific ligand binding, or also when embedded in the cell membranes. The dependence of the spontaneous formation on the concentration in the cell is hence a factor of the volume of the compartment in which the αSyn is formed, as well the net number of αSyn proteins. It has been shown that the amount of cross-linked αSyn dimers varies between different cell types and different sub-cellular compartments with varying volumes, in which the αSyn proteins resided(23). Additionally, it has been shown that over-expressing cells introduce more αSyn dimers and oligomers. Overall, it may well be that there are other more specific factors in the cell that stabilize or destabilize αSyn noncovalent dimer formation. Nevertheless, as a first step, its spontaneous formation depends on whether it is found in cells in effective concentrations of a few micromolars. This first stage in the αSyn oligomerization is important as it can serve as the precursor of the dityrosinate-linked covalent dimer(25) that is pivotal in the oxidative-stress pathway of Parkinson's disease(24).

Experimental procedures

Expression & purification of recombinant αSyn variants

The expression and production of recombinant αSyn variants (WT & Cys mutants given to us as a gift; see Acknowledgements) was similar to the protocol introduced by Grupi & Haas(8). Briefly, αSyn was expressed from a pT7-7 plasmid encoding either the WT or the single Cys mutant proteins. BL21 (DE3)-competent cells (Novagen) were grown in LB in the presence of ampicillin (0.1 mg/ml). Cells were induced with IPTG (Sigma) when cultures reached an $OD_{\lambda=600\ nm}$={0.6–0.7}, cultured at 37°C for 5 h, and harvested by centrifugation at 6000 rpm. The cell pellet was resuspended in lysis buffer which contains: 30 mM Tris–HCl, 2 mM ethylenediaminetetraacetic acid (EDTA) with 2 mM dithiotreitol (DTT) at pH 8.0 (also called buffer A) and 40 % sucrose, stirred for 20 minutes at room temperature. Then the solution was transferred to 50 mL tubes and centrifuged for 0.5 hour at 11,000 rpm. The cell pellet was re-suspended in dissolution buffer containing: 37 µL $MgCl_2$ dissolved in excess and 90 mL of buffer A to perform osmotic shock. DNA was precipitated by adding streptomycin sulfate (Sigma) to a final concentration of 10 mg/mL, and the mixture was stirred for 20 minutes at room temperature. After centrifugation at 12,000 rpm for 0.5 hour, the supernatant was collected and proteins were precipitated by ammonium sulfate (Sigma) at 300 mg/mL. The solution was stirred for 30 minutes at room temperature and centrifuged again at 12,000 rpm. The pellet was resuspended in buffer A and centrifuged with 100 kDa molecular weight cutoff (MWCO) Amicon tube (to remove aggregates and large oligomers) and then dialyzed using 8 kDa MWCO dialysis bags in at 4°C against buffer A overnight. The solution was

loaded on a 1 mL MonoQ column (GE Healthcare) using an FPLC system (Äkta Explorer), and αSyn was eluted with a salt gradient from 0 to 500 mM NaCl. The presence of αSyn in the fractions was verified by measuring absorption spectrum in the wavelength range 260-350 nm and running the samples in a 12 % SDS-PAGE Gel. Gels were then strained by fast seeBand (Gene Bio-application). Relevant fractions were unified and dialyzed against 8 kDa MWCO dialysis bags at 4°C against buffer A overnight. The molecular mass of the recombinant αSyn was verified by intact protein mass determination (see details in the next section). The purity of the αSyn was evaluated by running 12 % SDS-PAGE Gel. 12 % Native PAGE gel was used to probe the presence of Dimers. Protein samples were stored at -20°C

Intact protein mass determination

Proteins were dissolved in 40 % acetonitrile, 0.3 % formic acid (all solvents were MS-grade) at a concentration of 2-5 mg/mL. Then, the dissolved proteins were injected directly via a HESI-II ion source into a Q Exactive Plus (Thermo Fisher Scientific) mass spectrometer and a minimum of three scans lasting 30 seconds were obtained. The scan parameters were: scan range 1,800 to 3,000 m/z without fragmentation; resolution 140,000; positive polarity; AGC target $3x10^6$; maximum inject time 50 ms; spray voltage 4.0 kV; capillary temperature 275°C; S-lens RF level 55. Scan deconvolution was done using Mag Tran version 1.0.3.0 (Amgen).

AIEX-MALS experiments

AIEX-MALS experiments were performed using the same setup as was previously reported(26, 27). Briefly, we used a miniDAWN TREOS multi-angle light scattering detector, with three angle detectors (43.6°, 90°, and 136.4°) and a 658.9 nm laser beam (Wyatt Technology, Santa Barbara, CA) with a Wyatt QELS dynamic light scattering module for determination of hydrodynamic radius and an Optilab T-rEX refractometer (Wyatt Technology) set in-line with a 1 mL Mono-Q analytical column (GE, Life Science, Marlborough, MA). Experiments were performed using an Äkta Pure M25 system with a UV-900 detector (GE) adapted for analytical runs. All experiments were performed at room temperature (25°C) at 1.5 mL/min, using 30 mM Tris-HCl buffer pH = 8, as equilibration buffer, and 30 mM Tris-HCl buffer pH = 8 with 500 mM NaCl as elution buffer. 1 mg of αSyn at 0.2 mg/mL were injected to the column. Wash with 20 column volumes (CVs) of 0 % elution buffer and 7 CVs of 30 % elution buffer and eluted by 30 CVs gradient of 30-100 % elution buffer collecting 1 mL fractions. Data collection and AIEX-MALS analysis were performed using the ASTRA 6.1 software (Wyatt Technology). The refractive index of the solvent was defined as 1.331, and the viscosity was defined as 0.8945 cP (common parameters for PBS buffer at 658.9 nm). dn/dc (the refractive index increment with protein concentration) value for all samples was defined as 0.185 mL/g (a standard average value for proteins).

αSyn dye labeling

ATTO 488 and ATTO 647N (ATTO-TEC, GmbH) linked to iodoacetamide thiol-reactive groups, were coupled specifically to single Cys residues in αSyn mutants via a thiol coupling reaction. Thiols of Cys residues in samples of αSyn Cys mutants were reduced by 2 mM dithiotreitol (DTT, Sigma) for 1 hour in room temperature. Then DTT was removed by three rounds of dialysis against buffer A, using dialysis bags with 3 kDa MWCO. Then, the Cys thiols were further activated by 50 μM Tris(2-carboxyethyl)phosphine hydrochloride (TCEP, Sigma) for an additional one hour in room temperature. Then each dye was added to a separate vials, containing the protein, at a 5:1 dye:protein molar ratio. With ATTO 647N, 20 % dimethyl sulfoxide (DMSO, Sigma) was also added, to aid in dissolving the dye. The reaction mixtures were stirred for three hours at room temperature in the dark. Then, the reaction was terminated by adding 2 mM DTT, to react with the leftover dyes. Leftover dyes were then removed from the solution via three rounds of dialysis against buffer A, using dialysis bags with 3 kDa MWCO. Labeling products were then purified with a C-18 semi-preparative reversed-phase HPLC column. Labeled proteins were distinguished from free dyes that were not

removed by dialysis, by comparison of the chromatogram to the chromatogram of a free dye. Eluted labeling products were then brought to pH 8.0 immediately using high concentration Tris buffer, and the additional acetonitrile was removed using speed-vac. Pure labeling products were then assessed for their concentration, following the absorption of the dyes (ATTO 488/647N with an absorption coefficient of 90,000/150,000 $M^{-1}cm^{-1}$). The labeling products were then further characterized by 12 % SDS-PAGE gels molecular mass.

This labeling protocol has also been used for blocking the free thiol of the Cys residue in the Y39C αSyn mutant with iodoacetamide (IAA), only with a molar excess of IAA relative to the proteins.

FCCS-FRET and PIE smFRET measurements and analyses

All FCCS-FRET & PIE smFRET measurements were performed at a temperature of 37°C. The measurements of αSyn were performed in solutions of buffer A.

Both FCCS-FRET and PIE smFRET measurements were performed on a confocal fluorescence microscope (MicroTime200, PicoQuant GmbH Berlin, Germany) assembled on top of a modified Olympus IX71 inverted microscope stand. Pulsed picosecond diode lasers were used to excite the donor and acceptor (LDH-P-C-470B and LDH-P-C-640B, respectively, PicoQuant GmbH Berlin Germany) with output wavelengths of 470 nm and 640 nm, respectively (60 and 40 μW average-power at the sample, respectively). The conservation of polarization modes before reaching the sample was verified for both laser sources. Bandpass filters ensured that only light within the desired excitation band reached the sample. The repetition rate was set to 20 MHz. A dichroic beam splitter with high reflectivity at 470 & 635 nm reflected the light through the optical path to a high numerical aperture (NA) super Apo-chromatic objective (60X, NA=1.2, water immersion, Olympus, Japan), which focused the light onto a small confocal volume. Fluorescence from the excited molecules was collected through the same objective, and focused with an achromatic lens (f = 175 mm) onto a 50 μm diameter pinhole. The fluorescence emissions of the donor and the acceptor were separated using a dichroic long pass filter with the dividing edge at 605 nm (FF605-Di01, Semrock Rochester NY, USA). Emission that passed through the donor channel was selected with a 520/35 nm band-pass filter (FF01-520/35-25, Semrock Rochester NY, USA); the emission passed to the acceptor channel was selected by a 690/70 nm band-pass filter (HQ690/70, Chroma Technology Corp. Rockingham Vermont, USA). The detectors used were single photon avalanche photodiodes (SPAD) (Donor Channel: 100 μm, MPD PD1CTC, Acceptor Channel: 170 μm, Perkin Elmer SPCM-AQRH 13). The data were correlated by the HydraHarp400 Time Correlated Single Photon Counting (TCSPC) system and collected with SymphoTime version 5 (both by PicoQuant GmbH Berlin, Germany). The fluorescence decay curves were recorded as TCSPC histograms with bin widths of 16 ps.

Recorded data was stored in the time tagged time resolved (t3r) format, allowing each detected photon to be recorded together with its individual timing relative to the beginning of the measurement, and relative to the time of the excitation pulse, as well as the detection channel. The presented measurements were performed at an approximate depth of 70 μm inside a drop of solution, enclosed between two glass coverslips, sealed by a silicon double sticky sheet (Sigma). The total acquisition time varied from several minutes (mostly for FCS & FCCS measurements) to 1 hour (for PIE-smFRET measurements). A typical measurement included supporting measurements for setup and sample characterization, impulse response function (IRF) measurement using the reflection from a mirror on top of the microscope stage (FWHM of 656, 1,024 & 832 ps for 470 nm excitation with detection on the MPD SPAD, for 470 nm excitation with detection on the Perkin Elmer SPAD and for 635 nm excitation with detection on the Perkin Elmer SPAD, respectively), calibration of the effective excitation volume (2.0±0.1 fL) by measuring freely diffusing fluorescent molecules with a known diffusion coefficient (D=400 $\mu m^2/s$ at a temperature of 25°C for ATTO 488 for the donor detection

channel(40)). Each value was interpolated for room temperature (37°C), and for measurement of freely diffusing singly labelled αSyn molecules with either a donor or acceptor in order to characterize the correction of the intensities for FRET.

For PIE-smFRET, resulting acquisition files were converted into the universal photon HDF5 file format using the Pythin code *phconvert*(56). Then, single molecule burst analysis was carried out as described previously (57, 58) using the *FRETbursts* python software(59). For selecting all bursts (Fig. 5, A), we used a burst selection threshold of 50 photons in a burst. For selecting only bursts exhibiting fluorescence arising from donor excitation and from acceptor excitation (Fig. 5, B), we used a burst threshold of 25 photons from the donor excitation period & 25 photons from the acceptor excitation period.

Bulk FRET measurements

Acceptor excitation spectra were recorded using a spectrofluorometer (Jasco FP-8200ST, Japan), scanning excitation wavelength in the range 400-650 nm and focusing on acceptor emission at λ=665 nm. Acceptor excitation spectra were normalized to the excitation spectrum part, in the wavelength range for direct acceptor excitation (550-650 nm; see Fig. S8). Then, the excitation spectra part in the wavelength range that covers donor excitation (440-550 nm; see Fig. S8) served as a reporter for FRET.

Acknowledgements

We would like to thank Dr. Asaf Grupi, Dr. Dan Amir & Dr. Elisha Haas from the Mina & Everard Goodman Faculty of Life Sciences in Bar Ilan University for sharing the plasmids of αSyn bearing single cysteine mutations. We would also like to thank Dr. Asaf Grupi for fruitful discussions regarding αSyn. We would like to thank Dr. Nikolay Dokholyan from the Departments of Pharmacology, Biochemistry & Molecular Biology, Chemistry, and Biomedical Engineering at The Pennsylvania State University, for fruitful intellectual discussions. We would like to thank Dr. Yuval Garini from the Institute for Nanotechnology and Advanced Materials in Bar Ilan University for inviting us to perform the FCCS-FRET and PIE-smFRET measurements on his experimental setup. We would also like to thank Dr. William Breuer from the Proteomics and Mass Spectrometry Unit in the Alexander Silberman Institute of Life Sciences, the Hebrew University of Jerusalem, for assisting us with intact protein mass spectrometry.

Conflict of interest

The authors declare no conflict of interest with the contents of this article.

References

1. Recchia, A., Debetto, P., Negro, A., Guidolin, D., Skaper, S. D., and Giusti, P. (2004) α-Synuclein and Parkinson's disease. *FASEB J.* **18**, 617–626

2. Spillantini, M. G., Schmidt, M. L., Lee, V. M.-Y., Trojanowski, J. Q., Jakes, R., and Goedert, M. (1997) α-Synuclein in Lewy bodies. *Nature*. **388**, 839–840

3. Burré, J., Sharma, M., Tsetsenis, T., Buchman, V., Etherton, M. R., and Südhof, T. C. (2010) α-Synuclein Promotes SNARE-Complex Assembly in Vivo and in Vitro. *Science (80-.).* **329**, 1663 LP – 1667

4. Baba, M., Nakajo, S., Tu, P. H., Tomita, T., Nakaya, K., Lee, V. M., Trojanowski, J. Q., and Iwatsubo, T. (1998) Aggregation of alpha-synuclein in Lewy bodies of sporadic Parkinson's disease and dementia with Lewy bodies. *Am. J. Pathol.* **152**, 879–884

5. Goedert, M. (2001) Alpha-synuclein and neurodegenerative diseases. *Nat. Rev. Neurosci.* **2**, 492–501

6. Wakabayashi, K., Yoshimoto, M., Tsuji, S., and Takahashi, H. (1998) α-Synuclein immunoreactivity in glial cytoplasmic inclusions in multiple system atrophy. *Neurosci. Lett.* **249**, 180–182

7. Smith, B. R., Santos, M. B., Marshall, M. S., Cantuti-Castelvetri, L., Lopez-Rosas, A., Li, G., van Breemen, R., Claycomb, K. I., Gallea, J. I., Celej, M. S., Crocker, S. J., Givogri, M. I., and Bongarzone, E. R. (2014) Neuronal inclusions of alpha-synuclein contribute to the pathogenesis of Krabbe disease. *J. Pathol.* **232**, 509–521

8. Grupi, A., and Haas, E. (2011) Segmental Conformational Disorder and Dynamics in the Intrinsically Disordered Protein α-Synuclein and Its Chain Length Dependence. *J. Mol. Biol.* **405**, 1267–1283

9. Ingelsson, M. (2016) Alpha-Synuclein Oligomers-Neurotoxic Molecules in Parkinson's Disease and Other Lewy Body Disorders. *Front. Neurosci.* **10**, 408

10. Rao, J. N., Jao, C. C., Hegde, B. G., Langen, R., and Ulmer, T. S. (2010) A Combinatorial NMR and EPR Approach for Evaluating the Structural Ensemble of Partially Folded Proteins. *J. Am. Chem. Soc.* **132**, 8657–8668

11. Ulmer, T. S., Bax, A., Cole, N. B., and Nussbaum, R. L. (2005) Structure and Dynamics of Micelle-bound Human α-Synuclein. *J. Biol. Chem.* . **280**, 9595–9603

12. Ferreon, A. C. M., Gambin, Y., Lemke, E. A., and Deniz, A. A. (2009) Interplay of alpha-synuclein binding and conformational switching probed by single-molecule fluorescence. *Proc. Natl. Acad. Sci. U. S. A.* **106**, 5645–5650

13. Fusco, G., Chen, S. W., Williamson, P. T. F., Cascella, R., Perni, M., Jarvis, J. A., Cecchi, C., Vendruscolo, M., Chiti, F., Cremades, N., Ying, L., Dobson, C. M., and De Simone, A. (2017) Structural basis of membrane disruption and cellular toxicity by α-synuclein oligomers. *Science (80-.).* **358**, 1440 LP – 1443

14. Tsigelny, I. F., Sharikov, Y., Wrasidlo, W., Gonzalez, T., Desplats, P. A., Crews, L., Spencer, B., and Masliah, E. (2012) Role of alpha-synuclein penetration into the membrane in the mechanisms of oligomer pore formation. *FEBS J.* **279**, 1000–1013

15. Binolfi, A., Theillet, F.-X., and Selenko, P. (2012) Bacterial in-cell NMR of human α-synuclein: a

disordered monomer by nature? *Biochem. Soc. Trans.* **40**, 950 LP – 954

16. Bartels, T., Choi, J. G., and Selkoe, D. J. (2011) α-Synuclein occurs physiologically as a helically folded tetramer that resists aggregation. *Nature*. **477**, 107–110

17. Wu, K.-P., and Baum, J. (2010) Detection of Transient Interchain Interactions in the Intrinsically Disordered Protein α-Synuclein by NMR Paramagnetic Relaxation Enhancement. *J. Am. Chem. Soc.* **132**, 5546–5547

18. Frimpong, A. K., Abzalimov, R. R., Uversky, V. N., and Kaltashov, I. A. (2010) Characterization of intrinsically disordered proteins with electrospray ionization mass spectrometry: conformational heterogeneity of alpha-synuclein. *Proteins*. **78**, 714–722

19. Dettmer, U., Newman, A. J., Luth, E. S., Bartels, T., and Selkoe, D. (2013) In Vivo Cross-linking Reveals Principally Oligomeric Forms of α-Synuclein and β-Synuclein in Neurons and Non-neural Cells. *J. Biol. Chem.* . **288**, 6371–6385

20. Fauvet, B., Kamdem, M. M., Fares, M.-B., Desobry, C., Michael, S., Ardah, M. T., Tsika, E., Coune, P., Prudent, M., Lion, N., Eliezer, D., Moore, D. J., Schneider, B., Aebischer, P., El-Agnaf, O. M., Masliah, E., and Lashuel, H. A. (2012) Alpha-synuclein in the central nervous system and from erythrocytes, mammalian cells and E. coli exists predominantly as a disordered monomer. *J. Biol. Chem.*

21. Zhang, Y., Hashemi, M., Lv, Z., Williams, B., Popov, K. I., Dokholyan, N. V, and Lyubchenko, Y. L. (2018) High-speed atomic force microscopy reveals structural dynamics of α-synuclein monomers and dimers. *J. Chem. Phys.* **148**, 123322

22. Lv, Z., Krasnoslobodtsev, A. V., Zhang, Y., Ysselstein, D., Rochet, J.-C., Blanchard, S. C., and Lyubchenko, Y. L. (2015) Direct Detection of α-Synuclein Dimerization Dynamics: Single-Molecule Fluorescence Analysis. *Biophys. J.* **108**, 2038–2047

23. Coelho-Cerqueira, E., Carmo-Goncalves, P., Pinheiro, A. S., Cortines, J., and Follmer, C. (2013) alpha-Synuclein as an intrinsically disordered monomer--fact or artefact? *FEBS J.* **280**, 4915–4927

24. Krishnan, S., Chi, E. Y., Wood, S. J., Kendrick, B. S., Li, C., Garzon-Rodriguez, W., Wypych, J., Randolph, T. W., Narhi, L. O., Biere, A. L., Citron, M., and Carpenter, J. F. (2003) Oxidative Dimer Formation Is the Critical Rate-Limiting Step for Parkinson's Disease α-Synuclein Fibrillogenesis. *Biochemistry*. **42**, 829–837

25. van Maarschalkerweerd, A., Pedersen, M. N., Peterson, H., Nilsson, M., Nguyen, T., Skamris, T., Rand, K., Vetri, V., Langkilde, A. E., and Vestergaard, B. (2015) Formation of covalent di-tyrosine dimers in recombinant α-synuclein. *Intrinsically Disord. proteins*. **3**, e1071302–e1071302

26. AU - Some, D., AU - Amartely, H., AU - Tsadok, A., and AU - Lebendiker, M. (2019) Characterization of Proteins by Size-Exclusion Chromatography Coupled to Multi-Angle Light Scattering (SEC-MALS). *JoVE*. doi:10.3791/59615

27. Amartely, H., Avraham, O., Friedler, A., Livnah, O., and Lebendiker, M. (2018) Coupling Multi Angle Light Scattering to Ion Exchange chromatography (IEX-MALS) for protein characterization. *Sci. Rep.* **8**, 6907

28. Huang, C., Ren, G., Zhou, H., and Wang, C. (2005) A new method for purification of recombinant human α-synuclein in Escherichia coli. *Protein Expr. Purif.* **42**, 173–177

29. Ren, G., Wang, X., Hao, S., Hu, H., and Wang, C. (2007) Translocation of α-Synuclein Expressed in Escherichia coli. *J. Bacteriol.* **189**, 2777 LP – 2786

30. Folta-Stogniew, E., and Williams, K. R. (1999) Determination of molecular masses of proteins in solution: Implementation of an HPLC size exclusion chromatography and laser light scattering service in a core laboratory. *J. Biomol. Tech.* **10**, 51–63

31. Cho, M.-K., Nodet, G., Kim, H.-Y., Jensen, M. R., Bernado, P., Fernandez, C. O., Becker, S., Blackledge, M., and Zweckstetter, M. (2009) Structural characterization of alpha-synuclein in an aggregation prone state. *Protein Sci.* **18**, 1840–1846

32. Weinreb, P. H., Zhen, W., Poon, A. W., Conway, K. A., and Lansbury, P. T. (1996) NACP, A Protein Implicated in Alzheimer's Disease and Learning, Is Natively Unfolded. *Biochemistry*. **35**, 13709–13715

33. Stephens, A. D., Nespovitaya, N., Zacharopoulou, M., Kaminski, C. F., Phillips, J. J., and Kaminski Schierle, G. S. (2018) Different Structural Conformers of Monomeric α-Synuclein Identified after Lyophilizing and Freezing. *Anal. Chem.* **90**, 6975–6983

34. Curtain, C. C., Kirby, N. M., Mertens, H. D. T., Barnham, K. J., Knott, R. B., Masters, C. L., Cappai, R., Rekas, A., Kenche, V. B., and Ryan, T. (2015) Alpha-synuclein oligomers and fibrils originate in two distinct conformer pools: a small angle X-ray scattering and ensemble optimisation modelling study. *Mol. Biosyst.* **11**, 190–196

35. Tyn, M. T., and Gusek, T. W. (1990) Prediction of diffusion coefficients of proteins. *Biotechnol. Bioeng.* **35**, 327–338

36. Armstrong, J. K., Wenby, R. B., Meiselman, H. J., and Fisher, T. C. (2004) The hydrodynamic radii of macromolecules and their effect on red blood cell aggregation. *Biophys. J.* **87**, 4259–4270

37. Uversky, V. N. (1993) Use of fast protein size-exclusion liquid chromatography to study the unfolding of proteins which denature through the molten globule. *Biochemistry*. **32**, 13288–13298

38. Weidemann, T., and Schwille, P. (2013) Chapter Three - Dual-Color Fluorescence Cross-Correlation Spectroscopy with Continuous Laser Excitation in a Confocal Setup. in *Fluorescence Fluctuation Spectroscopy (FFS), Part A* (Tetin, S. Y. B. T.-M. in E. ed), pp. 43–70, Academic Press, **518**, 43–70

39. V, Buschmann; Kapusta, P; Koberling, F; Konig, M; Kramer, B; Ruttinger, S; Tannert, S; Veiga, M; Erdmann, R; Ortmann, U. (2014) Fluorescence lifetime correlation spectroscopy (FLCS) - a powerful tool for measuring diffusion, concentrations and interactions. url: https://www.picoquant.com/images/uploads/downloads/webtalk_flcs.pdf

40. Culbertson, C. T., Jacobson, S. C., and Michael Ramsey, J. (2002) Diffusion coefficient measurements in microfluidic devices. *Talanta*. **56**, 365–373

41. Elson, E. L., and Magde, D. (1974) Fluorescence correlation spectroscopy. I. Conceptual basis and theory. *Biopolymers*. **13**, 1–27

42. Blom, H., Chmyrov, A., Hassler, K., Davis, L. M., and Widengren, J. (2009) Triplet-State Investigations of Fluorescent Dyes at Dielectric Interfaces Using Total Internal Reflection Fluorescence Correlation Spectroscopy. *J. Phys. Chem. A.* **113**, 5554–5566

43. Kask, P., Piksarv, P., Pooga, M., Mets, U., and Lippmaa, E. (1989) Separation of the rotational contribution in fluorescence correlation experiments. *Biophys. J.* **55**, 213–220

44. Widengren, J., Mets, U., and Rigler, R. (1995) Fluorescence correlation spectroscopy of triplet states in solution: a theoretical and experimental study. *J. Phys. Chem.* **99**, 13368–13379

45. Müller, B. K., Zaychikov, E., Bräuchle, C., and Lamb, D. C. (2005) Pulsed Interleaved Excitation. *Biophys. J.* **89**, 3508–3522

46. Laurence, T. A., Kong, X., Jäger, M., and Weiss, S. (2005) Probing Structural Heterogeneities and Fluctuations of Nucleic Acids and Denatured Proteins. *Proc. Natl. Acad. Sci. U. S. A.* **102**, 17348–17353

47. Kapanidis, A. N., Laurence, T. A., Lee, N. K., Margeat, E., Kong, X., and Weiss, S. (2005) Alternating-Laser Excitation of Single Molecules. *Acc. Chem. Res.* **38**, 523–533

48. Lee, N. K., Kapanidis, A. N., Wang, Y., Michalet, X., Mukhopadhyay, J., Ebright, R. H., and Weiss, S. (2005) Accurate FRET Measurements within Single Diffusing Biomolecules Using Alternating-Laser Excitation. *Biophys. J.* **88**, 2939–2953

49. Ingargiola, A. (2017) Applying Corrections in Single-Molecule FRET. *bioRxiv*. 10.1101/083287

50. Wood, S. J., Wypych, J., Steavenson, S., Louis, J.-C., Citron, M., and Biere, A. L. (1999) α-Synuclein Fibrillogenesis Is Nucleation-dependent: implications for the pathgenesis of Parkinson's disease. *J. Biol. Chem.* **274**, 19509–19512

51. van Raaij, M. E., van Gestel, J., Segers-Nolten, I. M. J., de Leeuw, S. W., and Subramaniam, V. (2008) Concentration Dependence of α-Synuclein Fibril Length Assessed by Quantitative Atomic Force Microscopy and Statistical-Mechanical Theory. *Biophys. J.* **95**, 4871–4878

52. Horrocks, M. H., Tosatto, L., Dear, A. J., Garcia, G. A., Iljina, M., Cremades, N., Dalla Serra, M., Knowles, T. P. J., Dobson, C. M., and Klenerman, D. (2015) Fast Flow Microfluidics and Single-Molecule Fluorescence for the Rapid Characterization of α-Synuclein Oligomers. *Anal. Chem.* **87**, 8818–8826

53. Braitbard, M., Schneidman-Duhovny, D., and Kalisman, N. (2019) Integrative Structure Modeling: Overview and Assessment. *Annu. Rev. Biochem.* **88**, 113–135

54. Brodie, N. I., Popov, K. I., Petrotchenko, E. V, Dokholyan, N. V, and Borchers, C. H. (2019) Conformational ensemble of native α-synuclein in solution as determined by short-distance crosslinking constraint-guided discrete molecular dynamics simulations. *PLoS Comput. Biol.* **15**, e1006859–e1006859

55. Szabo, A., Schulten, K., and Schulten, Z. (1980) First Passage Time Approach to Diffusion Controlled Reactions. *J. Chem. Phys.* **72**, 4350–4357

56. Ingargiola, A., Laurence, T., Boutelle, R., Weiss, S., and Michalet, X. (2016) Photon-HDF5: An Open File Format for Timestamp-Based Single-Molecule Fluorescence Experiments. *Biophys. J.* **110**, 26–33

57. Lerner, E., Ingargiola, A., and Weiss, S. (2018) Characterizing Highly Dynamic Conformational States: The Transcription Bubble in RNAP-Promoter Open Complex as an Example. *J. Chem. Phys.* **148**, 123315

58. Ingargiola, A., Weiss, S., and Lerner, E. (2018) Monte-Carlo Diffusion-Enhanced Photon Inference: Distance Distributions And Conformational Dynamics In Single-Molecule FRET. *J. Phys. Chem. B*. 10.1021/acs.jpcb.8b07608

59. Ingargiola, A., Lerner, E., Chung, S., Weiss, S., and Michalet, X. (2016) FRETBursts: An Open Source Toolkit for Analysis of Freely-Diffusing Single-Molecule FRET. *PLoS One*. **11**, e0160716

Figures

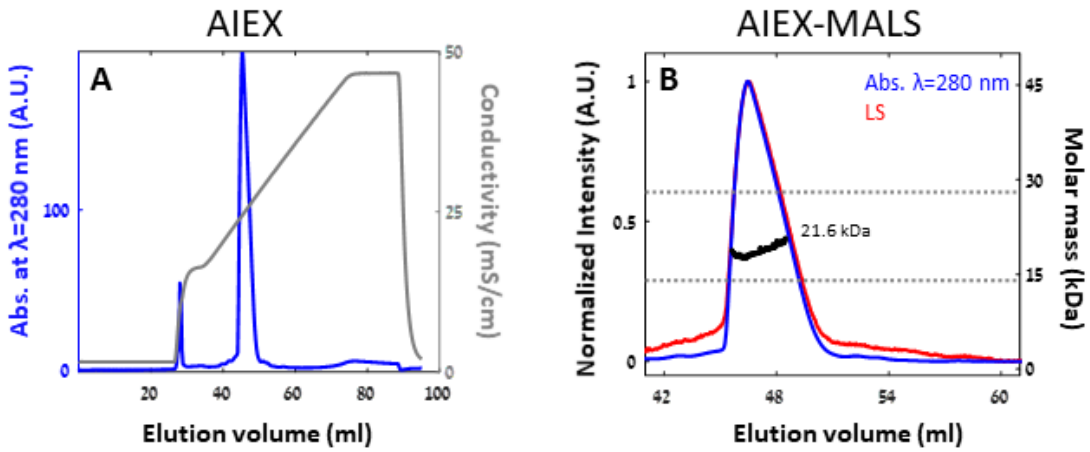

Figure 1: AIEX-MALS of WT αSyn elutes as a single peak with a molecular mass larger than αSyn monomer. A - AIEX using a 1 mL mono Q column with the gradient shown in grey, has been performed on a sample of the WT αSyn. The sample has eluted as a single elution peak (absorption at a wavelength of 280 nm, blue). B – the absorption at 280 nm (blue) and the light scattering intensity (red) were used for the calculation of MALS-derived molecular weight of 21.6±0.8 kDa. The elutant had a molecular mass value between that expected for an αSyn monomer and that expected for a dimer (dotted grey lines).

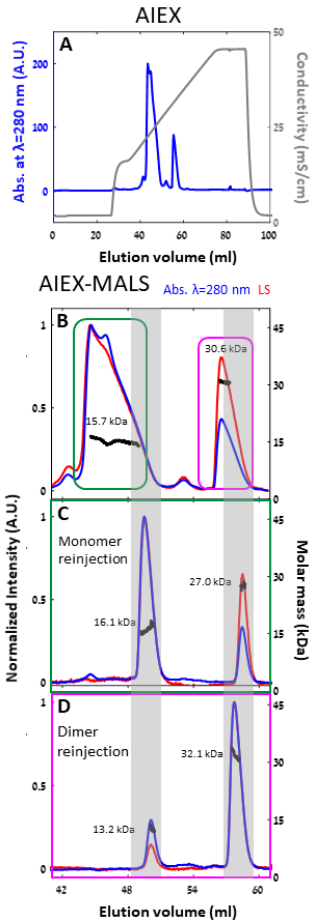

Figure 2: AIEX-MALS shows Y39C αSyn mutant has two peaks: monomer and dimer in equilibrium. A - AIEX using a 1 mL mono Q column with the gradient shown in grey, has been performed on a sample of Y39C αSyn mutant. The sample has eluted as two elution peaks (absorption at a wavelength of 280 nm, blue). B – the absorption at 280 nm (blue) and the light scattering intensity (red) were used for the calculation of MALS-derived molecular mass of 15.7±0.5 and 30.6±0.2 kDa, for the elution peaks labeled in green and magenta, characteristic of αSyn monomers and dimers, respectively. The monomer elution volume labeled in green was re-injected for another AIEX-MALS round and yielded two elution peaks with MALS-derived molecular mass 16.1±0.9 and 27.0±0.4 kDa (C). The dimer elution volume labeled in magenta (B) was re-injected for another AIEX-MALS round and yielded two elution peaks with MALS-derived molecular mass 13.2±0.5 and 32.1±0.9 kDa (D). The grey shades mark the elution volume range in which the re-chromatogrammed peaks of the monomer and dimer peaks were eluted. Note that while the dimer was eluted at similar elution volume range (compare grey shades in C and D to magenta label in B), the monomer was eluted at an elution volume range that is the high edge of the initial monomer elution peak (compare grey shades in C and D to green label in B).

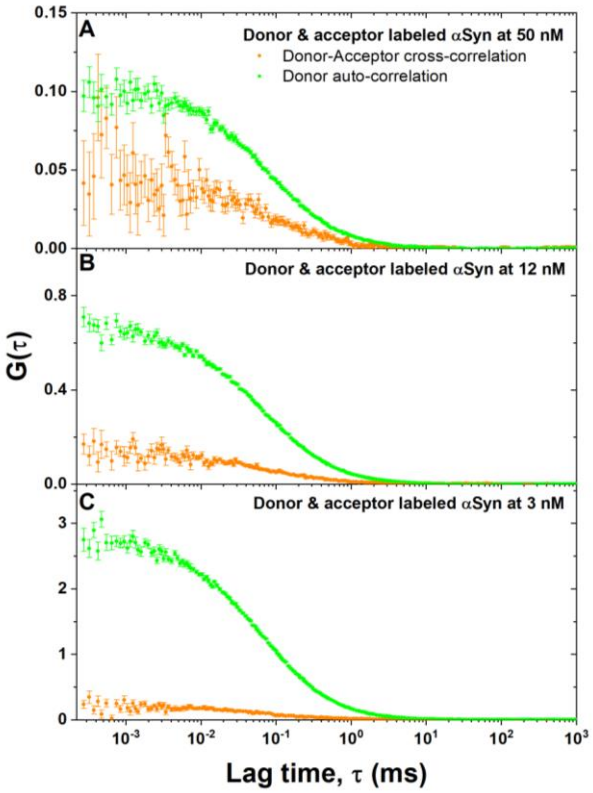

Figure 3: the abundance of a dimer or a short oligomer is decreasing with decreasing αSyn concentration. Donor fluorescence auto-correlation curves (green) and donor-acceptor fluorescence cross-correlation curves (orange) of donor- and acceptor-labeled αSyn Y39C mutants are shown at decreasing nominal concentrations (A-50 nM; b – 12.5 nM; c – 3.125 nM). The amplitude of the donor-acceptor fluorescence cross-correlation relative to the amplitude of the donor fluorescence auto-correlation decreases with decreasing αSyn concentration, indicative of a decreasing concentration of species having coincidence of both donor and acceptor fluorescence (namely dimers and short oligomers).

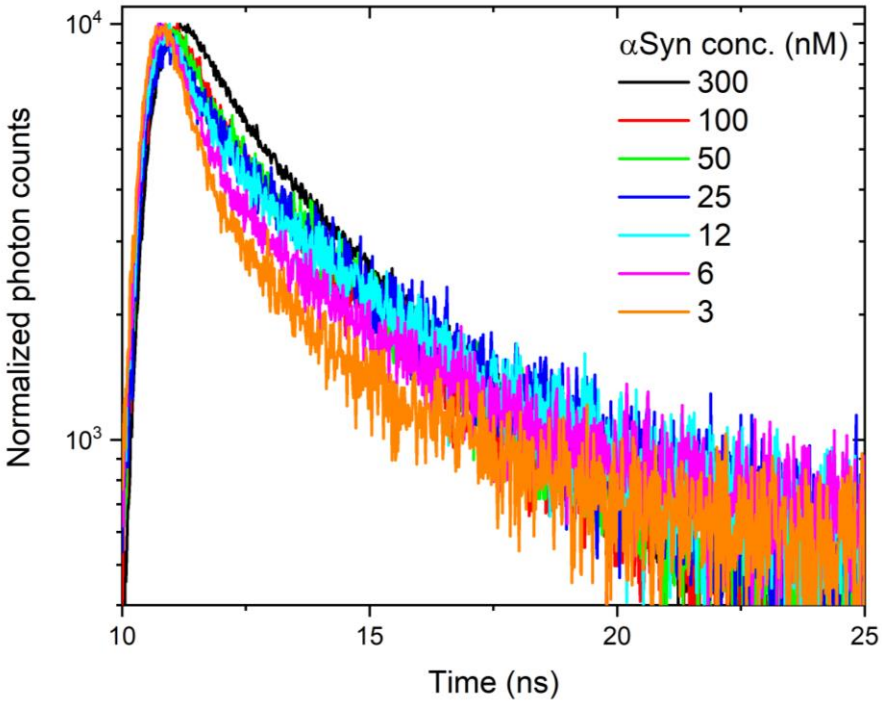

Figure 4: a signature of intermolecular FRET in acceptor fluorescence decay, decreases with αSyn concentration. The acceptor fluorescence decays, following donor excitation, were measured in donor- and acceptor-labeled Y39C αSyn mixtures at different nominal αSyn concentration (see inset). The fluorescence decay curves exhibit two components: a fast component, that is most probably due to leakage of the donor fluorescence red edge into the acceptor detection channel (see Fig. S12) and a slow component, indicative of acceptor excitations that were delayed in the donor excited state prior to the FRET event. The amplitude of the slow component is decreasing as the nominal αSyn concentration decreases.

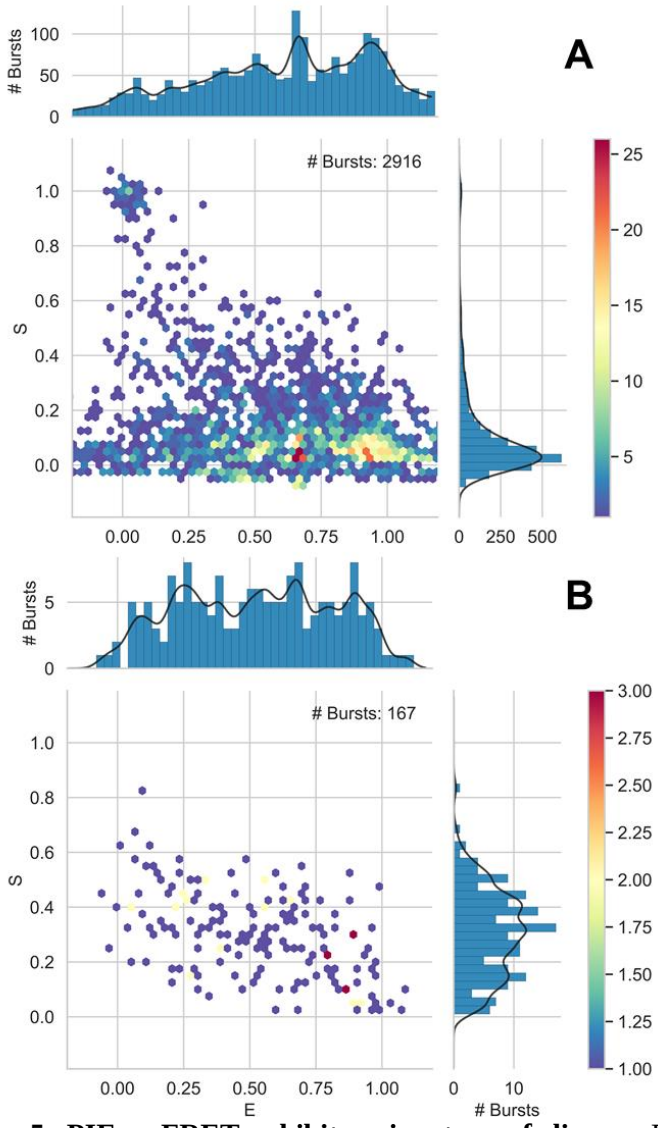

Figure 5: PIE-smFRET exhibit a signature of dimers. Donor- and acceptor-labeled Y39C αSyn mutants at a nominal concentration of 100 pM, were measured for 1 hour. A - Selection of all bursts with a total amount of photons higher than 50 show that the majority of bursts were αSyn monomers, with apparent stoichiometry ratio (S) values close to 0 (acceptor only) and 1 (donor only). B – selection of all bursts that had a total of more than 25 photons arising from donor excitation and more than 25 photons arising from acceptor excitation show a few bursts with different values of mean apparent FRET efficiencies (E), and a apparent S values lower than 0.5, characteristic of dimers, before applying correction factors (after applying corrections, S should be ~0.5).